tetragonal, orthorhombic terms in the Hamiltonian, but it is not obviously the highest in energy, d_{z^2} being more likely. A simple explanation then of the *observed* configuration is that the transition $4p_x \leftarrow 3d_{xz}$ is of low energy, and a large CI component arising from the state produced by the single excitation $4p_x \leftarrow 3d_{xz}$ is included in the final nickel ground state.

Conclusion

The electron density in $Ni(NH_3)_4(NO_2)_2$, as measured by these X-ray diffraction experiments, shows features around the nickel atom due to both aspherical d-electron distribution and more diffuse electron density. The ligand electron densities are qualitatively similar to those measured in other metal ammines[5] and nitro complexes.[32]

A quantitative analysis of the electron density by means of an aspherical valence-shell refinement allows more quantitative conclusions to be drawn. These are in general accord with simple ligand-field theory. The electron distribution in the nitro group closely resembles calculations of that in the free nitrite anion, except that 0.38 (8) electron have been σ donated to the metal atom. The π system is much less affected by complexation. The ammonia molecule, as expected, is a much weaker σ donor (0.11 (6) electron). The distribution of density around the nickel atom is close to that predicted by ligand-field theory except for an anomalously low $3d_{xz}$ population and a large diffuse population, mainly in $4p_x$. This can be explained by invocation of configuration interaction, but the spectra of the system have not been sufficiently well examined to provide convincing evidence of this.

More detailed bonding models will be discussed in terms of this quantitative information and that arising from measurements of the spin density in the subsequent paper.

Acknowledgment. We are grateful to Associate Professor Allan White for his painstaking data collection and to Dr. E. N. Maslen for critical comments. This work was supported by funding from the Australian Research Grants Committee.

Registry No. $Ni(NH_3)_4(NO_2)_2$, 19362-26-6.

Supplementary Material Available: A list of observed and calculated structure factors (10 pages). Ordering information is given on any curent masthead page.

Covalent Bonding in *trans*-Tetraamminedinitronickel(II) Studied by Polarized Neutron Diffraction at 4.5 K

B. N. Figgis,*[1a] P. A. Reynolds,[1a] and R. Mason[1b]

Contribution from the School of Chemistry, University of Western Australia, Nedlands Australia 6009, and The School of Molecular Sciences, University of Sussex, Brighton, BN1 9QJ, England. *Received April 2, 1982*

Abstract: Magnetic structure factors (303) obtained from the polarized neutron diffraction experiment on $Ni(ND_3)_4(NO_2)_2$ are reported. They are analyzed by least-squares methods in terms of a model which employs the 3d and 4p orbitals of the nickel atom, sp hybrid orbitals on oxygen and nitrogen atoms, 1s orbitals on hydrogen atoms, and an "overlap" density in the Ni–N bonds. It is found that 27% of the spin of the molecule resides on the ligand groups, more on the nitro than the ammine. The nickel atom spin is, as expected, mainly in the e_g orbitals, but there is an appreciable spin in one of the 4p orbitals. There is strong evidence of σ-bonding interactions, including direct observation of the anticipated negative overlap populations. There is no evidence of π bonding. The results compare well with those obtained from the charge-density study. Together these two experiments allow a quite detailed account of the bonding in the complex, including that within the NO_2 groups, to be formulated. Comparison of the results with a simple MO/ligand-field theory is instructive, but it is obvious some features will only be reproduced by an extensive ab initio MO calculation. The spin distribution in the molecule is consistent with the weak magnetic exchange present in the compound, providing an exchange pathway including O···H–N hydrogen bonding is considered feasible.

In the preceding paper we presented an X-ray diffraction study of the electron density of *trans*-tetraamminedinitronickel(II). In this paper we present the spin density in this complex as determined by polarized neutron diffraction. We then discuss the implications of the results for the bonding in this first-row transition-metal complex with relatively covalent features.

Polarized neutron diffraction can be used to obtain magnetic structure factors $F_M(hkl)$ for paramagnetic crystals.[2] These are the Fourier components of the magnetization density, in the same way as X-ray diffraction structure factors are Fourier components of the electron density in the crystal. If the orbital contribution to the magnetization is small, which it is in this $^3A_{2g}$ ground-term complex, we can obtain from the F_M's a description of the spin density. The spin density is the *difference* between the charge densities of α and β spins. The electron density is, of course, the *sum* of these two quantities. Thus the techniques of X-ray diffraction and polarized neutron diffraction are entirely complementary.

For chemical interpretation, however, spin density has some advantage over electron density. Apart from spin-polarization effects, the only molecular orbitals to contribute to the spin density are the partially filled ones in the valence shell. The effect of the nonbonding core orbitals is small since they are very nearly spin paired. This is in contrast to charge density where a major contribution is from core orbitals which do not take part significantly in bonding. Bonding effects are, therefore, proportionately more obvious in the polarized-neutron than the X-ray diffraction experiment. This is often offset by the lesser precision and extent of the polarized neutron data.

The primary effect of chemical bonding in simple complexes is to transfer charge from ligand to metal via the doubly occupied bonding orbitals and from metal to ligand in the singly occupied antibonding orbitals. Overall there is a net *charge* transfer to the metal and a *spin* transfer from the metal ion onto the ligand. Since the spin transfer generally occurs within an antibonding molecular orbital, we expect to see three effects in the spin density in Ni-

(1) (a) University of Western Australia. (b) University of Sussex.
(2) (a) Brown, P. J.; Forsyth, J. B.; Mason, R. *Philos. Trans. R. Soc. London, Ser. B* **1980**, *290*, 481–495. (b) Figgis, B. N.; Reynolds, P. A.; Williams, G. A.; Mason, R.; Smith, A. R. P.; Varghese, J. N. *J. Chem. Soc., Dalton Trans.* **1980**, 2333–2338.

0002-7863/83/1505-0440$01.50/0

$(NH_3)_4(NO_2)_2$: (1) a reduction of the spin on the metal atom, (2) spin appearing on the ligand atoms, and (3) a reduction of spin in the metal–ligand bonds due to overlap densities. There will also be more detailed effects reflecting the d configuration of the metal, σ vs. π bonding, and so on; these are effects which can be now described with some precision.

Experimental Section

A 75% deuterated crystal of $Ni(NH_3)_4(NO_2)_2$ was produced[3] by recrystallizing the hydrogeneous compound,[4] twice, from a 5% w/w solution of NH_3 in D_2O. The partial deuteration serves to reduce the background incoherent scattering from protons.

The crystal was mounted with (101) normal to the magnetic field direction on the D3 normal-beam polarized neutron diffractometer at the High-flux reactor of the Institut Laue-Langevin, Grenoble. The flipping ratios of 661 reflections were measured, after centering with an ω scan, at a wavelength of 90.0 pm, a temperature of 4.5 K and a magnetic field of 4.6 T. A few flipping ratios were also measured at various temperatures down to 1.53 K. The 661 reflections corresponded to all accessible reflections with $(\sin\theta)/\lambda \leq 7$ nm^{-1}. The major experimental limitation was due to the small range of lifting angle, ν, available. The beam polarization was 0.9787 (6). The flipping ratio of a reflection, $R(hkl)$, is defined by

$$R(hkl) = I\uparrow(hkl)/I\downarrow(hkl)$$

$I\uparrow(hkl)$ and $I\downarrow(hkl)$ are the respective diffracted intensities with neutrons incident of spin parallel ($\uparrow$) and antiparallel ($\downarrow$) to the applied magnetic field. This measured quantity can be related to structure factors, for centrosymmetric crystals, by 1,[5] in which, for simplicity, we have omitted

$$R(hkl) = (F_N^2 + 2s^2F_NF_M + s^2F_M^2)/(F_N^2 - 2s^2F_NF_M + s^2F_M^2)$$

correction terms due to polarization and flipping efficiencies. $F_N(hkl)$ is the nuclear structure factor which is known from a previous unpolarized neutron diffraction experiment on a crystal from the same batch.[3] s is the sine of the angle between the scattering vector and the direction of crystal magnetization. Since all quantities but F_M are known, it may be extracted from this equation by solution of a quadratic equation. The choice of solution, from the two alternatives, is dictated by our expectation that the magnetization density is approximately centered on the nickel atom and is 3d-like in character. The choice is rarely ambiguous. We note that the $F_M(hkl)$'s obtained have a known phase, unlike the case of the X-ray diffraction experiment. In this crystal, extinction is expected to be negligible,[3] but multiple scattering effects may occur.[2b] Accordingly, no reflections with $F_N < 1.6 \times 10^{-14}$ m were studied. A comparison of equivalent reflections showed that the major source of error was counting statistics. After equivalents were averaged, 303 unique reflections remained and are listed in the Supplementary Material. The data gave $\sum\sigma(F)/\sum|F| = 0.11$. The errors in the F_M's include an estimate of 0.08×10^{-14} m for the error in F_N for each reflection. Reflections with $\sigma(R_M) > 0.20\ \mu_B$ ($\approx 0.05 \times 10^{-14}$ m) have been omitted as of insufficient accuracy. $\sigma(F_M)$ varies from 0.01 to 0.2 μ_B while F_M ranges up to 1.8 μ_B per unit cell. The static bulk magnetization ($F(000)$) at 4.6 T has been measured as 2.07 μ_B/cell at 4.2 K with $g = 2.18$ and isotropic.[6] We estimate the contribution of the spin density to the magnetization density by use of the dipole approximation for the orbital magnetization term:

$$F_{spin}(hkl) = F_M(hkl) - 2.07(g-2)/g\langle j_2\rangle_{3d3d}$$

where $\langle j_2\rangle_{3d3d}$ is as previously defined, an integral of the theoretical radial distribution function of the nickel 3d electrons. The correction term is small compared to $F_M(hkl)$.

Results

As in the previous paper, we shall fit our data to a model for the spin density by least-squares methods. The spin density in the $(Ni(NH_3)_4(NO_2)_2$ molecule is modeled as the sum of a series of hybrid atomic orbital densities. On the nickel atom we place five 3d and three 4p functions; on the ammonia nitrogen atom (N(2)) four sp^3 hybrids; on the hydrogen atoms, 1s functions; and on the nitro-group nitrogen atom (N(1)) and the oxygen atoms three sp^2 hybrids and one p_π orbital. The coordinate system is as before. We varied from its theoretical value the radial function for the nickel atom 3d orbitals only, since the small amounts of spin expected in the remainder of the orbitals will not define their radial dependencies well. The modeling on oxygen using sp^2 hybrids differs from that of sp hybrids used in the previous paper; such sp^2 hybridization allows a greater flexibility on O(1) and O(2) and was introduced to investigate the postulated nonlinear N–H···O magnetic exchange pathway.

This model gave a goodness-of-fit $\chi = 1.64$ and a weighted reliability factor $R_w(F) = 0.076$ when $R_w(F)$, defined in Table I, was minimized. We preferred a second refinement in which "overlap" populations centered midway along each N–N(1) and Ni–N(2) bond were included as variables. These were modeled by hydrogen 1s form factors. χ was reduced to 1.53 and $R_w(F)$ to 0.072. Allowing the overlap density to vary in position and radial extent produced little further improvement. The refinements and their results are summarized in Tables I and II. A list of calculated F_M's is included in the deposited material. Fourier difference maps derived from the observed and calculated F_M's show no significant features. The estimated error in the spin density, arising from the $\sigma(F_M)$'s, away from the nickel atom, is $\sigma(p) \sim 4$ spins nm^{-3}. This corresponds with the observed fluctuations in the Fourier difference map. The spin densities implied by the final model for the Ni–NO_2 and Ni–N(2)–N(1) plane are shown in Figure 1a and 1b. Note that the contours increase logarithmically and that the random error level is about the third contour. The reader should note that these maps, being model maps, have had random errors removed but conversely spurious features of small amplitude may have been introduced. As such these maps and the Fourier maps of the previous paper are *not* directly comparable—only the parameters of the models should be used in that way. It is worth noting that even though the polarized neutron data are certainly *less* precisely measured than the X-ray diffraction data, the final ligand populations and the

Table I. Refinement Results for the Model Employing the Atomic Hybrid Orbitals Described in Table II, Including "Overlap" Populations in Ni–N Bonds[a]

$(\sin\theta)/\lambda$ range, nm^{-1}	0–7.0
N_{obsd} = no. of observations	303
N_{var} = no. of variables	23
$R(F)$	0.108
$R_w(F)$	0.072
χ	1.53
$F(000)_{calcd}/F(000)_{obsd}$	1.03

[a] $R(F) = \Sigma||F_o| - |F_c||/\Sigma|F_o|$, $R_w(F) = (\Sigma[w(F_o - F_c)^2]/\Sigma[wF_o^2])^{1/2}$, $\chi = (\Sigma[w(F_o - F_c)^2]/(N_{obsd} - N_{var}))^{1/2}$, $w = \sigma(F_o)^{-2}$.

Table II. Valence Refinement Parameters (Atom Centered Hybrids plus Overlaps)

	Nickel		
$3d_{xy}$	0.87 (7)	$4p_x$	0.17 (6)
$3d_{yz}$	0.04 (4)	$4p_y$	0.07 (6)
$3d_{xz}$	−0.02 (7)	$4p_z$	−0.14 (7)
$3d_{z^2}$	0.84 (7)		
$3d_{x^2-y^2}$	−0.05 (6)		
radius 3d	0.92 (1)		
	Ammonia		
N(2)			
$sp^3(1)$	0.033 (9)	H(1)	
		1s	−0.001 (8)
$sp^3(2)$	−0.000 (7)	H(2)/H(3)	
		1s	0.026 (5)
$sp^3(3)/(4)$	−0.001 (4)		
overlap pop Ni–N(2)	−0.050 (11)		
	Nitrite ion		
N(1)		O(1)/O(2)	
$sp^2(1)$	0.104 (20)	$sp^2(1)$	0.005 (14)
$sp^2(2)/(3)$	−0.009 (14)	$sp^2(2)$	0.005 (8)
		$sp^2(3)$	0.004 (8)
p_π	−0.008 (7)	p_π	0.004 (8)
overlap pop Ni–N(1)	−0.067 (14)		

(3) Figgis, B. N.; Reynolds, P. A.; Williams, G. A.; Lehner, N. *Aust. J. Chem.* **1981**, *34*, 993–999.
(4) Soret, L.; Robineau, F. *Bull. Soc. Chim. Fr.* **1889**, *2*, 138–139.
(5) Marshall, W.; Lovesey, S. W. "Theory of Thermal Neutron Scattering"; Clarendon Press: Oxford, 1971; pp 324–341.
(6) (a) Figgis, B. N.; Murray, K. S.; Reynolds, P. A.; Wright, S. *Aust. J. Chem.*, in press. (b) Figgis, B. N.; Reynolds, P. A.; White, A. H.; Williams, G. A.; Wright, S. *J. Chem. Soc., Dalton Trans.* **1981**, 997–1003.

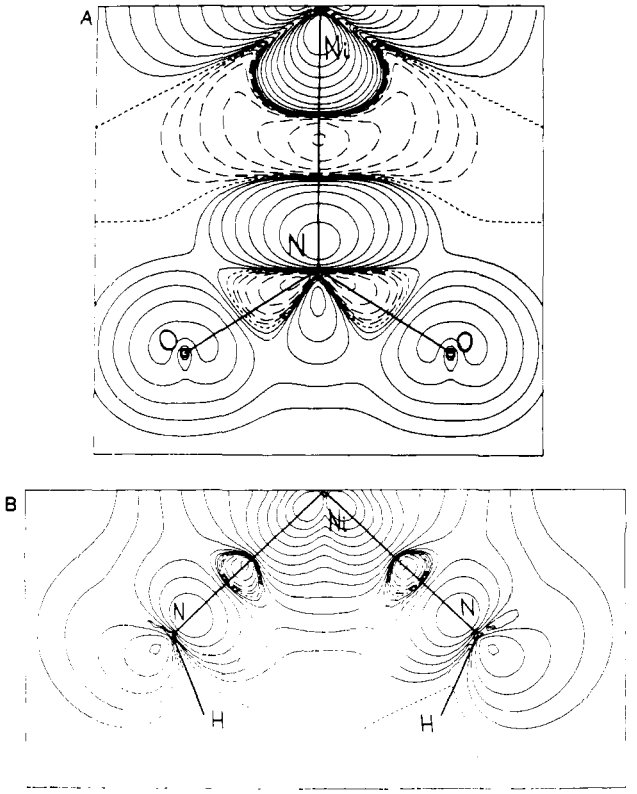

Figure 1. (A) Spin density of the fitted model in the *ac* plane, including the nickel and nitro groups. The contours are logarithmic: lowest, 1.64 spin nm^{-3}; highest (12th), 3400 spin nm^{-3}; increasing by factor 2. Positive, solid contour; negative, dashed; zero, dotted. (B) Spin density of the fitted model in the *bc** plane, including the nickel and the ammine N(2) and H(1).

implied covalent effects are *more* precisely estimated.

Discussion of Spin Density

Spin Transfers. From the data of Table II we can see that each ammonia ligand has a net spin of +0.082 (8) and each nitrite anion of one of +0.110 (14). The overlap population in the nickel–ammonia bond is −0.050 (11) and in the nickel–nitro bond −0.067 (14). The nickel spin population is 1.78 (6). The total spin populations are more precisely determined than individual hybrid populations, since the latter include a contribution from correlations in intraatomic populations.

There is, as expected, a reduction in the nickel atom population from two spins: the spin density delocalized onto the ligand atoms reflects the covalence. Concomitantly, we see a negative overlap density, reflecting the antibonding nature of the main contributing molecular orbital. The large spin population on the ligand molecules—27% of the total spin—reflects the much greater covalence in this complex relative to, for example, the $CoCl_4^{2-}$ ion[7] and the $Mn(H_2O)_6^{2+}$ ion[8] where the figures are 10% and 6%, respectively.

Nitrite Anion and Its Bonding to Nickel. If we break down the 0.110 (14) spins on each nitrite anion, we find that the π-electron system contains 0.000 (13) spins and the σ system 0.110 (20) spins, largely the spin is delocalized via σ antibonding. The bulk of the spin (0.104 (20)) resides in the σ antibonding nitro group lone pair, which is directed at the nickel atom. No other individual orbital has a significant population. The individual population on each oxygen atom, 0.016 (15), while positive, is hardly significant. The antibonding nature of the spin delocalized from the nickel atom is confirmed by the negative overlap population of −0.067 (14). This causes the spin density between Ni and N(1) to become small, reaching −8 spins nm^{-3} (which is negative at the 2σ level of significance). The net negative sign is evidence of the presence of spin polarization by the large positive nickel 3d population.

Ammonia and Its Bonding to Nickel. The 0.082 (8) spins on each ammonia molecule can be divided into two components: 0.033 (9) in the nitrogen atom lone pair and 0.026 (5) centered on H(2) and H(3). All other populations, including that on H(1), are not significant. The nitrogen atom lone pair population and the overlap population of −0.050 (11) shows that the spin is delocalized by σ antibonding.

The spin density nowhere reaches a significantly net negative value. There is a smaller amount of spin both on the ligand in total and on the N(2) lone pair compared to the nitro group. This reflects the smaller covalence expected from ammonia relative to the nitrite ion on the basis of considerations such as the spectrochemical series.

Nickel Atom. The configuration of the nickel atoms is $3d^{1.68(6)}4p^{0.10(6)}$, showing the presence of a diffuse population. The detailed d configuration is $d_{xy}^{0.87(7)}d_{yz}^{0.04(4)}d_{xz}^{-0.02(7)}d_{z^2}^{0.84(7)}d_{x^2-y^2}^{-0.05(6)}$, which we can compare with the simple crystal-field prediction of $d_{xy}^1d_{yz}^0d_{xz}^0d_{z^2}^1d_{x^2-y^2}^0$. The only significant spin populations are in d_{xy} and d_{z^2}, as expected. The reduction of the populations of d_{xy} and d_{z^2} from unity is caused by the spin delocalization onto the ligands through σ bonding.

Magnetic Exchange

A study of the temperature and field dependence of the powder and single-crystal susceptibilities and of the powder magnetization in this compound[6] has shown that there is weak intermolecular Heisenberg magnetic exchange. It occurs via pathways which do *not* form a three-dimensional net. If we assume this exchange occurs via the normal superexchange mechanism the shortest reasonable pathways are of the type Ni–N–O···H–N–Ni, that is the intermolecular step occurs via overlap of oxygen orbitals from a nitro group and hydrogen from an ammonia. While this pathway is long, the observed exchange *is* weak, and alternative pathways even longer. This O···H "hydrogen-bond" interaction has also been hypothesized[5] as the major component of the intermolecular energy of the crystal. The crystal structure[5] shows that these intermolecular bonds are of two types: those involving H(1) and those involving H(2) and H(3). Furthermore, the infrared spectrum[6b] shows both normal and anomalously weak N–H bonds. The charge-density study (previous paper) shows that the electron density around H(1) is *lower* than that around H(2) and H(3). This would cause overlap between O and H(1) to be less than between O and H(2) and H(3), and the magnetic exchange via pathways involving H(2) and H(3) to be stronger than those via H1. This implies a two-dimensional topology for the magnetic exchange, in agreement with the susceptibility and magnetization results.[6a]

If we now turn to the spin-density data, we see positive spin on all the atoms in the pathway Ni–N–O···H(2)–N–Ni (and correspondingly for H(3). The spin density on H(2) and H(3) is substantial 0.026 (5). In contrast, the spin density on H(1) is negligible (−0.001 (8)); there is therefore a "gap" in the pathway Ni–N–O···H(1)–N–Ni. It would appear that the polarized neutron experiment may be able to observe directly the magnetic-exchange pathway which one can only infer from the magnetic, X-ray diffraction, neutron diffraction, and infrared experiments.

Comparison of Spin and Charge Densities

The observed spin density, resulting from the polarized neutron diffraction experiment, implies that both the ammonia molecule and nitro groups are σ bonded to the nickel atom by donation of electrons from the nitrogen lone pairs. π bonding is much weaker. The nitro group is a stronger σ donor than than the ammonia molecule. This simple conventional picture of the molecular wave function is slightly complicated by the large spin density observed on two of the three ammonia hydrogen atoms. The σ-bonding electrons are donated to the nickel atoms d_{xy} and d_{z^2} orbitals as expected, but there is also evidence of 4p occupation.

(7) Figgis, B. N.; Reynolds, P. A.; Williams, G. A. *J. Chem. Soc., Dalton Trans.* **1980**, 2339–2352.
(8) Fender, B. E. F.; Figgis, B. N.; Forsyth, J. B.; Reynolds, P. A. *Proc. R. Soc. London*, submitted.

The charge density results from the X-ray diffraction experiment show a similar picture of σ-bonded ammonia molecules, more strongly σ-bonded nitro groups, with weaker, possibly negligible, π bonding. There is donation from the nitrogen atom lone pairs into the nickel atom $3d_{xy}$ and $3d_{z^2}$ orbitals. There are complications to that description. The σ donation from the nitro groups appears also to involve charge transfer from the oxygen atoms. The spin-density study shows a small, possibly not significant, positive spin population on the oxygen atoms. We must therefore postulate that while negative spin is transferred to the nickel atom from the nitro-nitrogen lone-pair atom, leaving positive spin behind, the resulting charge imbalance between nitrogen and oxygen atoms is reduced by migration of both positive and negative spin from O to N. Again the large $4p_x$ and small $3d_{xz}$ populations on the nickel atom are not reflected in the spin-density data. One could expect this result if spin is indeed restricted to the σ framework.

The qualitative agreement between the spin- and charge-density studies is therefore good, and it is pleasing to note that, while there is substantial overlap of conclusions, there are qualitative features in the spin density *not* predictable from charge density, and vice versa. Quantitative comparison should ideally be made via ab initio quantum mechanical calculations. Although this experiment has produced no definite evidence of spin-polarization effects, for the $CoCl_4^{2-}$ ion both the spin-density experiment and ab initio calculations show these effects.[9] This latter evidence, together with recent ab initio calculations on $Ni(NH_3)_4(NO_2)_2$,[9b] indicates that a comparison via simple ligand-field theory is of limited value. Nevertheless, it is instructive to make this comparison, because the charge-density results available for comparison are of good quality.

We write the bonding as of σ character, involving only nitrogen lone pair and $3d_{xy}$ and $3d_{z^2}$ nickel atom orbitals. Two bonding and two antibonding orbitals result. For the antibonding orbitals we write

$$\psi_a^1 = N_a^1[3d_{xy} - A_\sigma^{NH_3}/2(p_1 - p_2 + p_3 - p_4)]$$

$$\psi_a^2 = N_a^2[3d_{z^2} - A_\sigma^{NH_3}/(12)^{1/2}(-p_1 - p_2 - p_3 - p_4) - A_\sigma^{NO_2}/(12)^{1/2}(2p_5 + 2p_6)]$$

The bonding orbitals are derived from orthonormality considerations. The N's are normalizing constants; p_1 to p_4 are the ammonia nitrogen lone pairs; p_5 and p_6 the nitro-nitrogen lone pairs; $A_\sigma^{NH_3}$ the ammonia covalence parameter; $S_\sigma^{NH_3}$ the corresponding overlap; $A_\sigma^{NO_2}$, $S_\sigma^{NO_2}$ the corresponding nitro-nitrogen lone-pair parameters. We can use the ligand population, overlap population, and 3d populations (six observations) to derive, from the spin-density results, the four overlap and covalence parameters. The internal agreement is satisfactory. We obtained $A_\sigma^{NH_3} = 0.57$ (6); $S_\sigma^{NH_3} = \langle 3d|p\rangle = 0.08$; $A_\sigma^{NO_2} = 0.67$ (6); $S_\sigma^{NO_2} = 0.10$. We can compare these with the results for Co–Cl in $CoCl_4^{2-}$ viz., $A_\sigma^{Cl} = 0.15(5)$, $S_\sigma^{Cl} = 0.15$. We notice the much smaller covalence in the Co–Cl bond. The spectrochemical series gives $NO_2^- > NH_3 > Cl^-$, and also Ni(II) complexes would be expected to be more covalent than those of Co(II). The overlap S_σ^{Cl} is larger than $S_\sigma^{NO_2}$ and $S_\sigma^{NH_3}$, which are about equal in size as they should be for 3d N lone-pair overlaps at similar distances.

From these four parameters we can now calculate ligand charge-transfer overlap and 3d populations to compare with the observed charge-density results. We obtain for the ammonia-ligand charge-transfer and overlap populations 0.082 and 0.010. The values obtained from the X-ray experiment are 0.110 and 0.00 (not refined), respectively. For the nitro-ligand charge-transfer and overlap populations we obtain 0.110 and 0.013, which values are to be compared with 0.27 and 0.0 (not refined), respectively. For the 3d populations we have $3d_{xy} = 1.22$, $3d_{z^2} = 1.26$, which compare with 1.28 and 1.36, respectively.

The spin-density covalence parameters generally predict too little covalence relative to the charge-density results. Given the previous caveats and the involvement of the oxygen atoms in the bonding, the agreement is fair. An interesting point is the *small* overlap population expected in the charge density compared to the large values in the spin density cases (+0.010, +0.013 and −0.050, −0.067, respectively). The bonding overlap density is substantially less than the antibonding (negative) overlap density. This perhaps explains the lack of observable overlap density in the charge-density experiment from the Ni–N bonds.

If the overlap charge density is small in the Ni–N bonds then the observed radial extent (1.01 times theoretical) is much larger than for the spin density (0.92 (1)). Given the orbital populations, this implies that the nonbonded orbitals have a much *larger* radial extent (1.04) than the σ bonded (0.92). This is in line with our observations of the spin density in CrF_6^{3-}[10] (nonbonded 1.02 (1)), $CoCl_4^{2-}$ (bonded, 0.961 (5)),[7,9a] $CoBr_4^{2-}$ (bonded, 0.980 (4)),[11] and $Mn(H_2O)_6^{2+}$ (mixed nonbonded and strongly bonded 0.93).[8] These considerations suggest an antinephelauxetic effect: The stronger the bonding the more the 3d-like density around the metal contracts. In the optical spectra this effect may well be outweighed by the diffuse orbital population and by charge delocalization to and from the ligand producing a "traditional" nephelauxetic effect.

Acknowledgment. We thank the Institut Laue-Langevin for access to the D3 diffractometer and to Dr. P. J. Brown for invaluable assistance, and the Australian Research Grants Committee and the U. K. Science Research Council for support.

Registry No. $CHCl_2$, 3474-12-2; CH_3Cl, 74-87-3; CH_4, 74-82-8; CH_2Cl_2, 75-09-2; $CHCl_3$, 67-66-3; CCl_4, 56-23-5; CH_3CH_3, 74-84-0; CH_3CH_2Cl, 75-00-3; CH_3CHCl_2, 75-34-3; CH_3CCl_3, 71-55-6.

Supplementary Material Available: A listing of observed and calculated structure factors of unique reflections (6 pages). Ordering information is given on any current masthead page.

(9) (a) Chandler, G. S.; Figgis, B. N.; Phillips, R. A.; Reynolds, P. A.; Mason, R.; Williams, G. A. *Proc. R. Soc. London*, in press. (b) Chandler, G. S.; Phillips, R. A., unpublished results.

(10) Figgis, B. N.; Reynolds, P. A.; Williams, G. A. *J. Chem. Soc., Dalton Trans.* **1980**, 2348–2353.

(11) Figgis, B. N.; Reynolds, P. A.; Mason, R. *Proc. R. Soc. London*, in press.